J. Braz. Chem. Soc., Vol. 9, No. 6, 551-562, 1998.
Printed in Brazil.

0103 – 5053 $6.00 + 0.00

Article

Kinetic Analysis of the Gas-Phase Reactions of Methyl Vinyl Ketone with the OH Radical in the Presence of NO_X

André Silva Pimentel*, and Graciela Arbilla

Departamento de Físico-Química, Instituto de Química, Universidade Federal do Rio de Janeiro, Centro de Tecnologia – Bloco A – Sala 408, Cidade Universitária – 21949-900 Rio de Janeiro – RJ, Brazil

Received: September 1, 1998

Um mecanismo explícito para a reação do metil-vinil-cetona com radicais OH, numa mistura NO_x – ar, foi simulado resolvendo as equações diferenciais ordinárias usando o método Runge-Kutta-4-semi-implícito. Os resultados simulados são consistentes com os dados experimentais publicados e o modelo explica as principais vias de reação para a oxidação do MVK com radicais OH na presença de NO_x – ar. Usando uma análise dos autovetores e autovalores dos coeficientes de sensibilidade, para todas as espécies químicas envolvidas em diferentes tempos de reação, foi extraída informação cinética do sistema. Este método foi utilizado para reduzir o modelo cinético de forma objetiva. Foi utilizado, também, o método tradicional de análise de velocidade de produção (ROPA) para estudar a importância relativa das reações individuais. Usando a informação da análise de componente principal e da análise de velocidade de produção, foram identificadas as principais reações individuais.

An explicit chemical mechanism for the reaction of methyl vinyl ketone (MVK) with OH radicals in NO_x-air systems, was simulated by solving the corresponding ordinary differential equations using Runge-Kutta-4-semi-implicit method. The simulated results are consistent with the published experimental data and the model accounts for all the major pathways by which MVK reacts in NO_x-air systems. An eigenvalue-eigenvector analysis is used to extract meaningful kinetic information from linear sensitivity coefficients computed for all species of the chemical mechanism at several time points. This method is used to get an objective condition for constructing a minimal reaction set. Also, a classic method called rate of production analysis (ROPA) was used for the study of the reactions relevance. Using the principal component information as well as the rate of production analysis the main paths of reaction are identified and discussed.

Keywords: *principal component analysis, eigenvalue-eigenvector analysis, rate of production analysis, methyl vinyl ketone*

Introduction

Methyl vinyl ketone is the simplest α,β-unsaturated ketone. It is produced, together with methacrolein, from the gas-phase reactions of isoprene with the OH radical in the presence of oxides of nitrogen (NO_x)[1-3] and with O_3 [4,5]. The emissions of isoprene, which originate primarily from vegetation[6-11], may dominate over anthropogenic non-methane organic emissions on regional and global scales[12-14]. This potential environmental impact makes the inclusion of the isoprene atmospheric chemical reactions into airshed computer models necessary[15,16], which in turn requires a quantitative understanding of the atmospheric chemistry of both methacrolein and methyl vinyl ketone.

In this work, the gas-phase reactions of methyl vinyl ketone (hereafter MVK, $CH_3COCH=CH_2$) with OH radicals in NO_x-air systems are simulated and an eigenvalue-eigenvector analysis of the linear sensitivity coefficients, called Principal Component Analysis[17], is used to assess the relative importance of the elementary processes.

*e-mail: pimentel@iq.ufrj.br

Reaction rate analysis for complex kinetic systems includes the solution of the kinetic differential equations, the study of the effects of parameter changes on the results and the exploration of important reaction pathways[17-23]. This information is important to decide which reactions should be included in an atmospheric photochemical mechanism and, also, which reactions should be experimentally studied.

Only one experimental study has been conducted for the MVK reaction with OH radicals[24]. The authors of this study measured and identified the products of MVK oxidation, obtaining directly quantitative yields for glycolaldehyde ($HOCH_2CHO$), methylglyoxal (CH_3COCHO) and formaldehyde (HCHO). They also discussed and recommended a mechanism to represent the MVK + OH chemistry. Nevertheless, to our knowledge, a sensitivity analysis of the mechanism has not been done up to now.

In this paper the initial conditions for the simulations were those of the laboratory smog chamber experiments of Tuazon and Atkinson [24] in order to compare the calculated and experimental results.

The chemical mechanism

As previously discussed[24] MVK reacts essentially with OH radicals by H-atom abstraction, with an overall rate constant of 18.80×10^{-12} cm^3 $molecule^{-1}$ s^{-1} at 298 K[25].

The present chemical mechanism considers 28 species and 40 reactions and was proposed on the basis of reliable, previous models[26,27] and of the known MVK chemistry. Thermal rate constants were either taken from the literature[28-31] or estimated by comparison with similar compounds[32]. The photochemical reaction rates were estimated on the basis of the ethyl nitrite photodecomposition experimental data[24]. The chemical mechanism is listed in Table 1.

Methodology

The chemical process can be described by a system of kinetic differential equations,

$$\frac{\partial c(t)}{\partial t} = f(k, c(t))$$

where $c(t)$ is the n-vector of species concentrations with $c(t = 0) = c^0$ and k is the m-vector of kinetic parameters. Analytical solutions are not available for complex systems and a numerical solution is required. An important question in modeling studies is the effect of parameter change on the solution. In general, an alteration in the kinetic parameters from k^0 to k at time t_1 causes a change in the solution of the system at a time t_2 (with $t_2 > t_1$). The effect of the parameter change on the solution can be expressed through the first order local concentration sensitivity coefficients defined as

$$S_{ij}\,(k^0, c^0, t_1, t_2) = \frac{\partial\, c_i\,(t_2)}{\partial\, k_j}$$

The S_{ij} coefficient is the linear approximation of concentration change of species i at the time t_2 caused by the differential change of the parameter of reaction j at time t_1 from value k_j0 to k_j. In this work the parameters are the photochemical coefficients and the thermal rate constants.

Sensitivity coefficients are normalized in order to eliminate their dependence on the dimensions of the kinetic model. The effect of a single parameter on a group of concentrations is demonstrated by the overall sensitivities which are the sum of the squares of the normalized sensitivities. A better description of parameter-concentration interdependence consists in the identification of the groups of parameters which have joint influence on a group of concentrations. This type of information is given by the principal component analysis of the normalized sensitivity matrix. The eigenvectors of the matrix S^TS, where S is the array of sensitivity coefficients, identify parameter groups while the eigenvalues give information about the effectiveness of these parameter groups for the change of species concentrations. A parameter is considered important if it belongs to a large element of an eigenvector corresponding to a large eigenvalue. The methodology of numerical simulation, sensitivity and principal component analysis is fully discussed in the literature[33-38].

An alternative method for the study of the reactions relevance is the rate of production analysis called ROPA[35,39]. Although the combination of species reduction and rate sensitivity analysis[36] seems to be a more effective way for this purpose, the rate of production analysis is a classic method for the identification of important reaction pathways. This methodology requires the calculation of the Pij matrix elements[40,41], which show the contribution of reaction j to the rate of production of species i. The rate of production analysis is rather difficult to interpret in a correct way and must be analyzed together with principal component results.

Results and Discussions

The full mechanism and rate constants are presented in Table 1. The reduced mechanism was obtained after elimination of the non-important reactions (denoted by # in Table 1) on the basis of the principal component analysis described below. The rank of reactions ordered by overall sensitivities and rates is shown in Table 2. We calculated normalized sensitivities for all species at time points 1.9, 6.9, 11.9, 16.8, 21.8, 26.8, 33.8, 40.8 and 49.8 minutes. Eigenvalues of S^TS and the corresponding eigenvectors are listed in Table 3.

In the conditions of the modeling, the main source of hydroxyl radicals is the reaction (5) ($HO_2 + NO \rightarrow OH + NO_2$) which follows the photolysis of the ethyl nitrite

Table 1. Chemical Mechanism for Gas-Phase Reactions of MVK with the OH Radical in the Presence of NO_x.

Reactions	Rate Constants at 298 K Units of Molecule, cm^3, s
#1) $HONO + OH \rightarrow H_2O + NO_2$	$k_1 = 4.86\times10^{-12}$
#2) $OH + HNO_3 \rightarrow H_2O + NO_3$	$k_2 = 1.50\times10^{-13}$
3) $NO + OH \rightarrow HONO$	$k_3^a = 1.12\times10^{-11}$
4) $OH + NO_2 \rightarrow HNO_3$	$k_4^a = 1.34\times10^{-11}$
5) $HO_2 + NO \rightarrow OH + NO_2$	$k_5 = 8.28\times10^{-12}$
6) $NO + O_3 \rightarrow NO_2 + O_2$	$k_6 = 1.81\times10^{-14}$
7) $NO + NO_3 \rightarrow 2\ NO_2$	$k_7 = 2.60\times10^{-11}$
8) $NO_2 + O_3 \rightarrow NO_3 + O_2$	$k_8 = 3.23\times10^{-17}$
9) $HONO + h\nu \rightarrow OH + NO$	$j_9 = 1.63\times10^{-3}$
10) $NO_2 + h\nu + (O_2) \rightarrow NO + O_3$	$j_{10} = 4.26\times10^{-3}$
11) $HCHO + OH + (O_2) \rightarrow HO_2 + CO + H_2O$	$k_{11} = 9.57\times10^{-12}$
12) $CH_3CHO + OH + (O_2) \rightarrow CH_3CO_3 + H_2O$	$k_{12} = 1.58\times10^{-11}$
13) $CH_3O + (O_2) \rightarrow HCHO + HO_2$	$k_{13} = 4.59\times10^{4}$
14) $CH_3O_2 + NO \rightarrow NO_2 + CH_3O$	$k_{14} = 7.68\times10^{-12}$
15) $CH_3CO_3 + NO + (O_2) \rightarrow NO_2 + CH_3O_2 + CO_2$	$k_{15}^a = 9.98\times10^{-12}$
16) $CH_3CO_3 + NO_2 \rightarrow CH_3CO_3NO_2$	$k_{16} = 3.63\times10^{-12}$
17) $CH_3CO_3NO_2 \rightarrow CH_3CO_3 + NO_2$	$k_{17} = 1.81\times10^{-4}$
18) $CH_3CH_2O + O_2 \rightarrow CH_3CHO + HO_2$	$k_{18} = 9.48\times10^{-15}$
#19) $CH_3CH_2O + NO \rightarrow CH_3CH_2ONO$	$k_{19} = 4.40\times10^{-11}$ (k_∞)
20) $CH_3C(O)CH{=}CH_2 + OH + (O_2) \rightarrow 0.28\ CH_3C(O)CH(OH)CH_2O_2 + 0.72\ CH_3C(O)CH(O_2)CH_2OH$	$k_{20}^b = 1.88\times10^{-11}$
21) $CH_3C(O)CH(OH)CH_2O_2 + NO \rightarrow CH_3C(O)CH(OH)CH_2O + NO_2$	$k_{21}^c = 8.90\times10^{-12}$
22) $CH_3C(O)CH(OH)CH_2O \rightarrow CH_3C(O)CHOH + HCHO$	$k_{22}^c = 7.00\times10^{-3}$
23) $CH_3C(O)CHOH + O_2 \rightarrow CH_3C(O)CHO + HO_2$	$k_{23}^c = 1.59\times10^{-13}$
24) $CH_3C(O)CH(O_2)CH_2OH + NO \rightarrow CH_3C(O)CH(O)CH_2OH + NO_2$	$k_{24}^c = 8.90\times10^{-12}$
25) $CH_3C(O)CH(O)CH_2OH + (O_2) \rightarrow CH_3CO_3 + HOCH_2CHO$	$k_{25}^c = 8.50\times10^{4}$
26) $CH_3CH_2ONO + h\nu \rightarrow CH_3CH_2O + NO$	$j_{26}^c = 1.85\times10^{-4}$
#27) $2\ OH \rightarrow H_2O_2$	$k_{27} = 1.14\times10^{-11}$
#28) $H_2O_2 + OH \rightarrow H_2O + HO_2$	$k_{28} = 1.70\times10^{-12}$
29) $HO_2 + HO_2 \rightarrow H_2O_2 + O_2$	$k_{29} = 7.73\times10^{-12}$
30) $HO_2 + NO_2 \rightarrow HO_2NO_2$	$k_{30} = 2.33\times10^{-12}$
31) $HO_2NO_2 \rightarrow HO_2 + NO_2$	$k_{31} = 1.68\times10^{-1}$
32) $NO_2 + NO_3 \rightarrow N_2O_5$	$k_{32} = 6.56\times10^{-13}$
33) $N_2O_5 \rightarrow NO_2 + NO_3$	$k_{33} = 2.27\times10^{-2}$
#34) $CH_3O + NO \rightarrow CH_3ONO$	$k_{34} = 2.13\times10^{-11}$
#35) $CH_3O + NO_2 \rightarrow CH_3ONO_2$	$k_{35} = 8.75\times10^{-12}$
36) $CH_3O_2 + NO_2 \rightarrow CH_3O_2NO_2$	$k_{36} = 2.93\times10^{-12}$
37) $CH_3O_2NO_2 \rightarrow CH_3O_2 + NO_2$	$k_{37} = 1.698$
38) $HCHO + (2\ O_2) + h\nu \rightarrow 2\ HO_2 + CO$	$j_{38} = 1.76\times10^{-5}$
39) $HCHO + h\nu \rightarrow H_2 + CO$	$j_{39} = 2.66\times10^{-5}$
40) $CH_3CHO + (2\ O_2) + h\nu \rightarrow CH_3O_2 + HO_2 + CO$	$j_{40} = 3.53\times10^{-6}$

a- Reference 31; b- Reference 25; c- Estimated; d- References 28 and 29; # Non-important Reactions.

Table 2. Rank of Reactions by Overall Sensitivity and Rates.

Rank	Reaction	Overall Sens.*	Reaction	Rates**
1	26	6.23×10^{2}	30	1.26×10^{12}
2	20	2.15×10^{2}	31	1.26×10^{12}
3	4	1.47×10^{2}	10	6.24×10^{11}
4	16	9.50×10^{1}	6	4.91×10^{11}
5	15	8.90×10^{1}	32	4.06×10^{11}
6	5	4.04×10^{1}	33	3.95×10^{11}
7	9	3.14×10^{1}	8	1.24×10^{11}
8	10	2.18×10^{1}	7	1.13×10^{11}
9	6	1.85×10^{1}	36	4.28×10^{10}
10	14	1.79×10^{1}	37	4.28×10^{10}
11	3	1.75×10^{1}	5	3.15×10^{10}
12	8	1.37×10^{1}	26	2.56×10^{10}
13	22	1.32×10^{1}	18	2.56×10^{10}
14	7	1.24×10^{1}	16	2.54×10^{10}
15	30	1.12×10^{1}	20	1.40×10^{10}
16	31	1.09×10^{1}	25	1.01×10^{10}
17	13	9.59	24	1.01×10^{10}
18	18	9.03	4	9.42×10^{9}
19	23	9.00	17	9.25×10^{9}
20	25	9.00	12	6.56×10^{9}
21	24	9.00	22	4.05×10^{9}
22	21	9.00	23	4.05×10^{9}
23	36	8.94	21	3.92×10^{9}
24	37	8.93	11	1.72×10^{9}
25	29	8.80	39	9.97×10^{8}
26	32	6.87	14	7.89×10^{8}
27	33	4.46	13	7.67×10^{8}
28	12	1.79	38	6.59×10^{8}
29	17	1.39	15	4.91×10^{8}
30	40	1.08	40	3.05×10^{8}
31	38	1.01	9	2.93×10^{8}
32	11	5.59×10^{-1}	29	1.05×10^{8}
33	34	3.11×10^{-1}	3	5.54×10^{7}
34	35	1.05×10^{-1}	2	3.18×10^{7}
35	19	9.38×10^{-2}	35	2.14×10^{7}
36	1	4.56×10^{-2}	19	5.11×10^{6}
37	39	9.28×10^{-3}	1	4.17×10^{6}
38	27	2.17×10^{-3}	28	6.43×10^{5}
39	2	3.80×10^{-4}	34	3.67×10^{5}
40	28	1.21×10^{-4}	27	2.63×10^{2}

*undimensional; **units in molecule, cm^3 and s.

Table 3. Eigenvalues and eigenvectors for the MVK photooxidation mechanism.

Eigenvalues♣	1.13×10^3	6.70×10^1	4.83×10^1	4.36×10^1	3.69×10^1	1.94×10^1	1.72×10^1	1.43×10^1	1.20×10^1	1.07×10^1
Eigenvectors♠										
1	(26) .733	(5) -.583	(10) .394	(9) -.537	(9) .521	(26) -.433	(30) -.596	(20) .330	(22) -.841	(8) -.441
2	(20) .418	(10) -.417	(20) -.376	(14) -.384	(14) -.401	(5) -.386	(31) .590	(5) -.319	(18) -.301	(32) -.383
3	(4) -.346	(6) .387	(5) -.375	(3) .376	(3) -.274	(15) .333	(29) .273	(16) .288	(13) -.222	(7) .372
4	(16) -.269	(7) .284	(6) -.360	(20) -.288	(15) .274	(16) -.327	(20) -.257	(36) .288	(9) .217	(10) .357
5	(15) .260	(8) -.277	(26) .336	(16) -.278	(36) .267	(18) .255	(4) .205	(37) -.287	(26) .116	(6) -.307
6	(3) -.073	(29) .207	(9) -.256	(15) .258	(37) -.266	(13) -.232	(9) .190	(14) -.223	(3) .113	(33) .302
7	(5) -.061	(26) .185	(4) .243	(36) .240	(16) -.259	(4) -.226	(26) .126	(25) -.223	(10) .113	(22) .205
8	(8) .057	(32) -.146	(30) .179	(37) -.240	(4) .257	(14) .224	(18) -.105	(29) .218	(8) -.107	(13) -.194
9		(16) .122	(31) -.177	(5) .110	(5) -.173	(36) -.221	(8) .092	(15) -.207	(25) -.092	(23) -.152
10		(20) -.117	(7) -.154	(4) -.103	(30) .132	(37) .221	(7) -.080	(13) .206	(6) -.089	(21) -.131
11		(33) .114	(8) .125	(10) -.094	(31) -.131	(29) .174	(13) -.066	(23) -.201	(20) -.083	(24) -.131
12		(15) -.105	(24) .121	(6) .090	(26) -.108	(20) .130	(24) .061	(18) .193	(7) .083	(30) -.123
13		(30) .076	(21) .121	(30) -.079	(12) .106	(22) -.128	(21) .061	(22) -.183	(30) .059	(31) .121
14		(31) -.075	(32) .114	(31) .078	(22) .089	(3) .128	(25) .059	(10) .166	(31) -.058	(25) -.118
15		(4) .067	(22) .105	(13) -.075	(24) .085	(8) .102	(23) .057	(6) -.160	(12) -.056	(18) .067
16		(14) .051	(29) .088	(22) -.074	(21) .085	(7) -.094		(30) -.155		(16) -.066
17			(33) -.087	(17) .072	(13) -.073	(24) .079		(31) .154		(36) -.056
18			(14) .075	(40) .068	(8) -.070	(21) .079		(26) -.148		(37) .056
19			(12) .065		(20) -.062	(23) .056		(4) -.145		(29) .052
20			(13) -.053		(7) .056	(32) .053		(9) -.142		(14) .051
21					(25) .054			(21) .103		
22					(23) .050			(24) .103		
23					(40) .050			(3) -.057		

Eigenvalues♣	9.00	9.00	8.94	7.79	7.27	6.32	5.70	4.84	4.27	3.95
Eigenvectors♠										
1	(23) -.864	(24) .701	(25) -.788	(13) .438	(18) .778	(32) .473	(4) -.495	(15) .557	(14) .610	(16) -.426
2	(25) .375	(21) -.701	(13) -.384	(21) .420	(20) -.294	(33) -.400	(14) .369	(16) .415	(4) .403	(21) -.405
3	(13) -.213	(23) -.116	(22) .235	(24) .420	(25) -.207	(13) .392	(36) .332	(21) -.281	(16) -.321	(24) -.405
4	(32) .115		(32) .213	(32) -.283	(26) .202	(8) -.367	(37) -.331	(24) -.281	(13) .273	(15) -.378
5	(18) -.114		(18) -.207	(18) -.245	(23) -.199	(7) .316	(15) -.319	(13) .252	(36) .267	(8) .245
6	(33) -.098		(33) -.182	(33) .230	(5) .159	(18) -.231	(9) .276	(20) -.247	(37) -.267	(7) -.233
7	(21) .094		(23) -.133	(25) -.219	(22) -.157	(16) -.177	(20) -.254	(9) .238	(15) .160	(13) .232
8	(24) -.094		(6) .101	(23) -.217	(9) .155	(4) -.149	(3) .205	(3) .202	(9) -.138	(5) -.162
9	(22) .055		(10) -.099	(4) -.163	(13) .114	(36) -.142	(22) .197	(12) -.194	(25) -.136	(32) -.153
10	(6) .055		(40) .060	(3) .148	(32) .108	(37) .142	(13) -.164	(17) -.158	(23) -.134	(33) .139
11	(10) -.054			(20) -.129	(36) -.099	(14) -.131	(25) .110	(4) -.154	(22) -.128	(14) -.135
12				(16) -.128	(37) .099	(10) .115	(23) .104	(23) -.085	(20) .114	(29) .111
13				(9) .125	(33) -.097	(26) -.093	(16) -.068	(5) -.079	(40) -.098	(9) .111
14				(36) -.123	(8) -.090	(6) -.091	(21) .065	(14) .075	(8) -.077	(23) -.110
15				(37) .123	(16) -.089	(12) .078	(24) .065	(25) -.071	(7) .070	(17) .110
16				(22) .115	(29) -.086	(3) .061	(12) .058	(8) .070	(12) -.053	(25) -.103
17				(8) .077	(15) -.083	(15) -.058	(32) .057	(7) -.065		(20) -.096
18				(7) -.061	(7) .077	(25) .051	(33) -.051	(6) -.057		(3) .073
19				(15) .061	(12) -.069			(37) -.055		(18) -.067
20				(26) -.054	(24) .053			(36) .055		(26) -.051
21					(21) .053					
22					(6) .052					

Eigenvalues♣	1.60	1.41	7.45×10^{-1}	5.33×10^{-1}	1.46×10^{-1}	8.79×10^{-2}	7.41×10^{-2}	4.73×10^{-2}	2.08×10^{-2}	1.85×10^{-2}
Eigenvectors♠										
1	(3) .784	(29) .871	(12) .643	(12) -.628	(11) -.776	(17) .787	(6) .489	(33) .697	(34) .828	(38) -.751
2	(4) .369	(5) .393	(40) -.591	(40) -.590	(38) -.410	(40) -.499	(10) .437	(32) .573	(19) .298	(34) .412
3	(20) .358	(30) .195	(17) -.321	(17) -.364	(12) -.248	(11) -.228	(11) .383	(7) -.270	(11) -.262	(7) .181
4	(9) .240	(31) -.194	(38) -.251	(16) -.166	(6) .176	(38) .148	(7) -.354	(8) -.261	(38) .257	(6) -.179
5	(22) .099		(6) .114	(14) -.143	(34) -.147	(16) .147	(8) -.296	(6) .151	(17) -.199	(39) .177
6	(12) .094		(11) -.096	(13) -.140	(39) -.141	(15) .081	(33) -.254	(10) .113	(39) -.162	(17) .175
7	(26) .077		(22) -.081	(38) .115	(40) .133	(33) -.068	(32) -.211	(34) .059	(12) .094	(10) -.169
8	(15) -.074		(13) -.072	(15) -.103	(7) -.127	(39) -.064	(38) -.176		(27) -.067	(8) .162
9	(25) .074		(25) -.070	(6) -.075	(10) .117	(34) .061	(34) .171		(33) -.063	(11) .160
10	(18) .070		(7) -.069	(11) .068	(17) -.103	(32) -.058	(39) .156			(12) -.130
11	(23) .067		(23) -.064	(22) .057	(8) -.096	(10) .054	(12) -.113			(35) .126
12	(14) -.064		(34) -.062	(25) .055	(32) -.082	(19) .050				(33) .102
13	(16) .062		(15) .057	(7) .054	(33) -.078					(32) .076
14	(29) -.057			(23) .050						(1) .069

Eigenvalues♣	6.96×10^{-3}	2.14×10^{-3}	1.93×10^{-3}	1.32×10^{-3}	8.09×10^{-4}	4.61×10^{-4}	2.59×10^{-4}	2.18×10^{-5}	5.11×10^{-6}	2.42×10^{-6}
Eigenvectors♠										
1	(7) .534	(39) -.588	(39) -.632	(19) .674	(27) -.848	(1) .771	(31) -.673	(2) .993	(28) .996	(37) .706
2	(8) .498	(19) .468	(1) .516	(35) .585	(39) .246	(35) -.590	(30) -.665	(39) .063	(27) -.062	(36) .706
3	(10) .451	(27) -.447	(35) .411	(1) .300	(19) -.244	(39) .166	(27) -.235			(28) -.054
4	(6) .445	(35) -.265	(19) -.371	(34) -.235	(31) .211	(19) .122	(35) .136			
5	(33) .134	(38) -.234	(11) .115	(39) .209	(30) .209	(30) -.078	(19) -.124			
6	(32) .115	(11) .233	(27) .066	(11) -.055	(35) .149	(31) -.078	(39) .075			
7	(27) .106	(1) -.153	(2) .065	(7) .051	(1) .137		(38) .060			
8	(39) -.083	(34) -.151			(11) -.101					
9	(35) -.080	(17) .057			(38) .076					
10	(2) -.078				(7) .057					
11					(8) .054					
12					(28) -.054					
13					(6) .051					
14					(10) .051					

♣ Each column represents a principal component, that is a group of coupled reactions. The eigenvalues indicate the effectiveness of each group in changing the modeling results.

♠ First entry refers to the rate constant for the reaction listed in Table 1 and second entry lists eigenvector components. The eigenvectors give the relative importance of each reaction in the group.

($CH_3CH_2ONO + h\nu \rightarrow CH_3CH_2O + NO$) and the oxidation of the CH_3CH_2O radicals ($CH_3CH_2O + O_2 \rightarrow CH_3CHO + HO_2$). Reaction (5) accounts for *ca.* 92% of OH radical formed and the only significant sources of NO are the photodecomposition of ethyl nitrite (8%) and NO_2 (91%), reactions (26) and (10), respectively. Since we had no data on photolysis light intensities during the experiments, the ethyl nitrite photodecomposition coefficient was estimated from experimental data (Fig. 1) and values, which gave consistent results for other photodecompositions, were used. The photolysis rates were also consistent with the value reported in the literature[42] for NO_2 photodecomposition under the same experimental conditions. Also, photochemical reactions of other species, not including NO_2 photodecomposition, are of negligible importance compared with other paths. As expected, the set of reactions (Table 1) accounts for the MVK photooxidation in good agreement with experimental data (Fig. 3). As presented in Figs. 2 and 4, simulated results for the formation of the main products, glycolaldehyde, methylglyoxal and formaldehyde, show a slight deviation mainly for longer times.

In the simulation conditions, formaldehyde is formed both from acetaldehyde, the initial product of ethyl nitrite photolysis, reaction (26), and by the sequence of reactions initiated by OH radical oxidation of MVK:

$$CH_3C(O)CH{=}CH_2 + OH + (O_2) \rightarrow 0.28\ CH_3C(O)CH(OH)CH_2O_2 + 0.72\ CH_3C(O)CH(O_2)CH_2OH$$

The rate of production analysis shows that 63% of formaldehyde is formed through reaction (13), $CH_3O + (O_2) \rightarrow HCHO + HO_2$ and 37% through the reaction sequence (20), (21) and (22), which involve the reaction of $CH_3C(O)CH(OH)CH_2O_2$ with NO. Under the modeling conditions, the secondary reactions of formaldehyde are of minor importance. As observed experimentally[24,42], the formed formaldehyde reacts essentially with OH radicals which are in relatively high concentrations (calculated

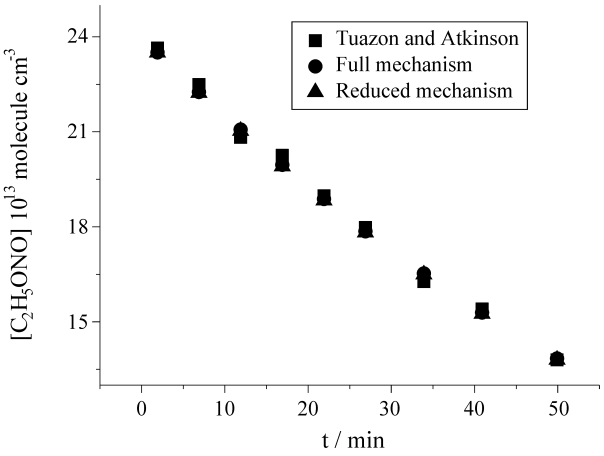

Figure 1. Simulated and experimental data for the ethyl nitrite photodecomposition as a function of reaction time.

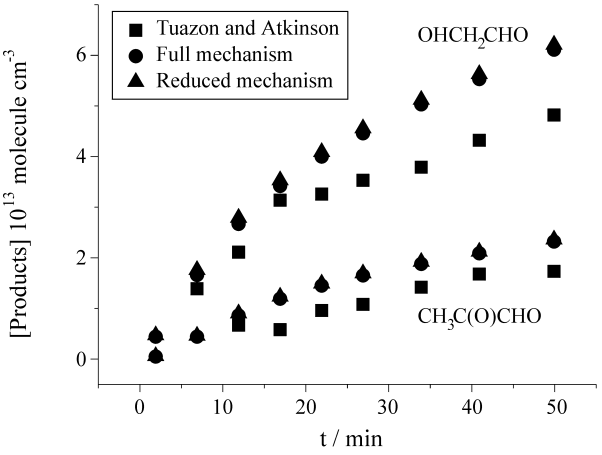

Figure 2. Simulated and experimental data for the main products of the gas-phase reactions of MVK with the OH radical in the presence of NO_x as a function of reaction time.

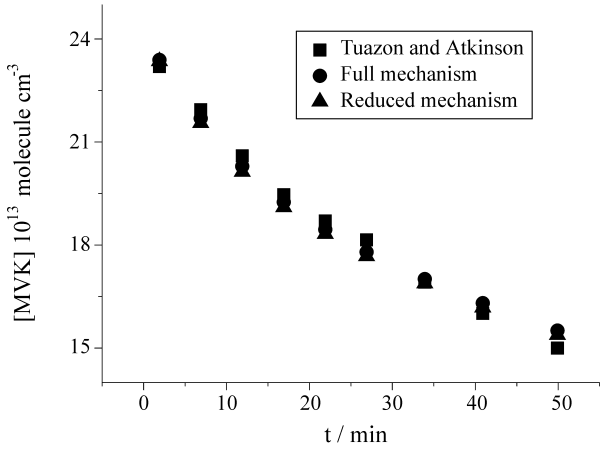

Figure 3. Simulated and experimental data for the oxidation of the MVK as a function of reaction time.

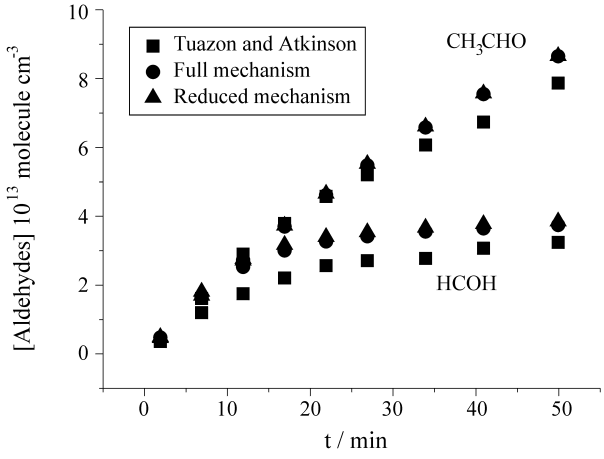

Figure 4. Simulated and experimental data for aldehyde concentrations as a function of reaction time.

values about 0.5-1.0 x 10^7 molecule cm^{-3}). Nevertheless, the rate of this reaction path is 5.1% of the total formation rate and, in comparison with OH radical reaction (11) ($HCHO + OH + (O_2) \rightarrow HO_2 + CO + H_2O$), the photochemical decompositions (39) and (40) ($HCHO + (2\ O_2) + h\nu \rightarrow 2\ HO_2 + CO$ and $HCHO + h\nu \rightarrow H_2 + CO$) are of non-negligible importance (26%).

In the conditions of this simulation, the formation of acetaldehyde (Fig. 4) and peroxyacetyl nitrate (PAN) (Fig. 5) can be attributed to the photooxidation of ethyl nitrite[42]. The simulated results are in good agreement with experimental data only for peroxyacetyl nitrate. The main discrepancy between the experimental results and the model predictions is higher concentrations of calculated acetaldehyde. The reasons for this discrepancy are not well established, but may be associated to the large uncertainty in the related kinetic parameters. In comparison with OH radical reaction ($CH_3CHO + OH + (O_2) \rightarrow CH_3CO_3 + H_2O$), the acetaldehyde photochemical decompositions ($CH_3CHO + (2\ O_2) + h\nu \rightarrow CH_3O_2 + HO_2 + CO$) are of non-negligible importance, as shown by the principal component analysis.

The 1st and 2nd principal components in Table 3 show that ethyl nitrite photodecomposition, reaction (26), oxidation of MVK, reaction (20), PAN chemistry, reactions (15) and (16), and OH/NO chemistry, reactions (3), (4) and (5), are strongly coupled and are the most influential reaction sequence in the mechanism. Thus, a small deviation in k_{20} or j_{26} should greatly affect the simulation results.

According to the magnitude of the eigenvalues and significant entries (≥ 0.20) of the corresponding eigenvector, the individual reactions may be classified in three groups:

1) Eigenvalues λ_1 to λ_{22} are much larger than the remaining ones. Note that $\sum_{i=1}^{22} \lambda_i \ / \ \sum_{j=1}^{40} \lambda_j$ = 0.9989. Principal components Ψ_1 to Ψ_{22} contain steps (3)-(10), (12)-(16), (18), (20)-(26), (29)-(33), (36) and (37), forming the "basic" part of mechanism. According to Ψ_1, the most influential reaction sequence is formed by (26), (20), (4), (16) and (15). This "reaction kernel" emphasizes that the largest effect is brought about by setting the parameters j_{26} and k_{20}. Reactions (4), (15) and (16) largely affects the NO/NO_2 ratio and the simulated results. Due to the coupling of the individual reactions, this ratio not only depends on the rate of reactions (20) and (26) but also on all the reactions involving NO_x. Since j_{26} is an estimated parameter, some deviations of the simulated results may be attributed to it. An uncertainty analysis of this parameter shows that a change of 10% in j_{26} leads to a substantial change of all product concentrations (6.8% in glycoaldehyde 9.8% in methylglyoxal and 7.3% in formaldehyde). The inclusion of another minor path of reaction, such as the formation of alkylnitrates, might affect the NO/NO_x ratios by a non-negligible amount.

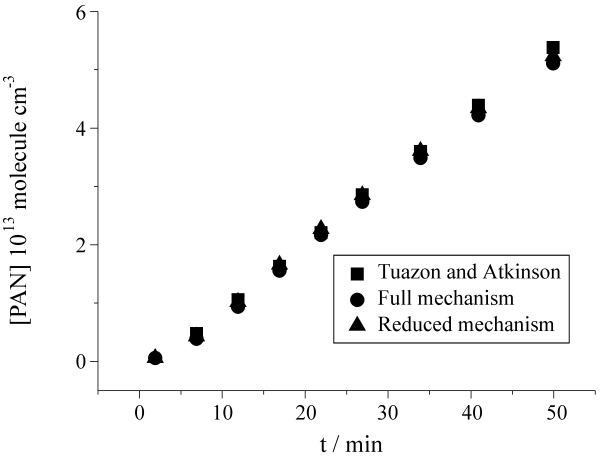

Figure 5. Simulated and experimental data for the peroxyacetyl nitrate (PAN) concentrations as a function of reaction time.

2) According Ψ_{23} to Ψ_{27}, reactions (11), (12), (17), (38) and (40), are of "transitional" importance. As it will be shown, in spite of their small contributions they can not be removed from the mechanism.

3) Reactions (1), (2), (19), (27), (28), (34), (35) and (39) contained in Ψ_{28} to Ψ_{41} with eigenvalues below 2.52×10^{-2} are unimportant and can be eliminated.

As shown in Table 4, eliminating the last group of reactions causes small changes in concentrations and only the HCHO concentration shows a deviation greater than others (8.8%) because of the elimination of reaction (39). If this reaction is included in the reduced mechanism, this deviation decreases to 2.89%. However, additional elimination of steps (11), (12), (17), (38) and (40) (*i.e.* reactions of "transitional" importance) leads to large deviations (Table 4). That is, no further reduction of the mechanism is possible since all concentration changes should be small.

The rank of reactions by overall sensitivity (Table 2) suggests that reaction 39 may be eliminated. However, this

Table 4. Comparison of concentration deviations from full mechanism, eliminating of steps (1), (2), (19), (27), (28), (34), (35) and (39) (column A) and also steps (11), (12), (17), (38) and (40) (column B).

	Deviations (%)	
Compounds	A	B
MVK	-0.87	-5.20
Ethyl Nitrite	-0.26	-0.26
Glycolaldehyde	1.58	9.49
Methylglyoxal	1.61	9.27
Formaldehyde	8.80	29.27
Acetaldehyde	0.14	17.90
PAN	2.51	-14.19

elimination leads to large deviations (*e.g.* at t = 49.9 min the deviation for HCHO is 8.8%). The rate reaction rank (Table 2) gives a different rank of reactions and is not an effective way of reducing a mechanism. Individual rates do not consider the interactions between reactions and may lead to incorrect conclusions about the relevance of individual reactions. Consequently, as previously shown the rate of production analysis is a good method for the exploration of the reaction pathways.

Conclusions

The mechanism of Table 1 is quite successful in reproducing chamber data for the oxidation of MVK by OH radicals. The rate of production analysis gives useful information in determining the main reaction pathways.

Rate of production results in combination with principal component analysis show that reaction are strongly coupled and confirm that the most influential reactions paths are the ethyl nitrite photolysis, the MVK oxidation and the chemistry of NO_x, PAN and OH radical. On the basis of the calculated eigenvalues, the mechanism can be reduced to 33 reactions. No further reduction is possible since all concentration changes should be small. Certainly, the conclusions taken from the eigenvalue-eigenvector analysis are only valid for the rather narrow range of conditions of the smog chamber experiments. However, the information seems useful for identifying a minimal reaction set and for assessing the relationships and dependencies among the parameters.

Since reactions (21) - (25) form the basic part of the mechanism, the estimation of their rate constants may lead to a considerable uncertainty in the simulated results. Thus, further experiments with this system, in order to study those reaction paths, would be important for the improvement of atmospheric photochemical mechanisms.

Acknowledgements

The authors gratefully acknowledge CAPES and FAPERJ for partial financial support, NCE/UFRJ for computing facilities on the SP2 supercomputer, and Prof. T. Turányi (Central Research Institute for Chemistry, Budapest, Hungary) for a free copy of the KINAL package.

Note

All calculations were performed using the KINAL package[43].

References

1. Arnts, R.R.; Gay Jr., B.W. In *Photochemistry of some naturally emitted hydrocarbons*, EPA-600 3-79-081, September, 1979.
2. Gu, C.L.; Rynard, C.M.; Hendry, D.G.; Mill, T. *Environ. Sci. Technol.* **1985**, *19*, 151.
3. Tuazon, E.C.; Atkinson, R. *Int. J. Chem. Kinet.* **1990**, *22*, 1221.
4. Kamens, R.M.; Gery, M.W.; Jeffries, H.E.; Jackson, M.; Cole, E.I. *Int. J. Chem. Kinet.* **1982**, *14*, 955.
5. Niki, H.; Maker, P.D.; Savage, C.M.; Breitenbach, L.P. *Environ. Sci. Technol.* **1983**, *17*, 312A.
6. Rasmussen, R.A. *Environ. Sci. Technol.* **1970**, *4*, 667.
7. Rasmussen, R.A. *J. Air Pollut. Control Assoc.* **1972**, *22*, 537.
8. Tingey, D.T.; Manning, M.; Grothaus, L.C.; Burns, W.F. *Physiol. Plants* **1979**, *47*, 112.
9. Zimmerman, P.R. In *Determination of emission rates of hydrocarbons from indigenous species of vegetation in the Tampa/St. Petersburg FL, area*, EPA-904/9-77-028, 1979.
10. Isidorov, V.A.; Zenkevich, I.G.; Ioffe, B.V. *Atmos. Environ.* **1985**, *19*, 1.
11. Lamb, B.; Westberg, H.; Allwine, G.; Quarles, T. *J. Geophys. Res.* **1985**, *90*, 2380.
12. Zimmerman, P.R.; Chatfield, R.B.; Fishman, J.; Crutzen, P.J.; Hanst, P.L.; *Geophys. Res. Lett.* **1978**, *5*, 679.
13. Lamb, B.; Guenther, A.; Gay, D.; Westberg, H. *Atmos. Environ.* **1987**, *21*, 1695.
14. Zimmerman, P.R.; Greenberg, J.P.; Westberg, C.E. *J. Geophys. Res.* **1988**, *93*, 1047.
15. Lloyd, A.C.; Atkinson, R.; Lurmann, F.W.; Nitta, B. *Atmos. Environ.* **1983**, *17*, 1931.
16. Killus, J.P.; Whitten, G.Z. *Environ. Sci. Technol.* **1984**, *18*, 142.
17. Vajda, S.; Valko, P.; Turányi, T. *Int. J. Chem. Kinet.* **1985**, *17*, 55.
18. Dickinson, R.P.; Gelinas, R.J. *J. Comp. Phys.* **1976**, *21*, 123.
19. Hwang, J.T.; Dougherty, E.P.; Rabitz, S.; Rabitz, H. *J. Chem. Phys.* **1978**, *69*, 5180.
20. Dougherty, E.P.; Hwang, J.T.; Rabitz, H. *J. Chem. Phys.* **1979**, *71*, 1794.
21. Edelson, D.; Allara, L. *Int. J. Chem. Kinet.* **1980**, *12*, 605.
22. Turányi, T.; Bérces, T.; Vajda, S. *Int. J. Chem. Kinet.* **1989**, *21*, 83.
23. Turányi, T. *J. Math. Chem.* **1990**, *5*, 203.
24. Tuazon, E.C.; Atkinson, R. *Int. J. Chem. Kinet.* **1989**, *21*, 1141.
25. Atkinson, R. *Atmos. Environ.* **1990**, *24A*, 1.
26. Pimentel, A.S.; Arbilla, G. *Química Nova* **1997**, *20*, 252.
27. Carter, W.P.L. *Atmos. Environ.* **1990**, *24A*, 481.
28. Atkinson, R. *J. Phys. Chem. Ref. Data* **1989**, Monograph n. 1, 1.
29. Atkinson, R. *J. Phys. Chem. Ref. Data* **1994**, Monograph n. 2, 1.

30. Atkinson, R.; Baulch, D.L.; Cox, R.A.; Hampson Jr., R.F.; Kerr, J.A.; Troe, J. *J. Phys. Chem. Ref. Data* **1992**, *21*, 1125.
31. Atkinson, R.; Baulch, D.L.; Cox, R.A.; Hampson Jr., R.F.; Kerr, J.A.; Troe, J.; *J. Phys. Chem. Ref. Data* **1989**, *18*, 881.
32. Atkinson, R. *Int. J. Chem. Kinet.* **1997**, *29*, 99.
33. Steinfeld, J.I.; Francisco, J.S.; Hase, W.L. In *Chemical Kinetics and Dynamics*, Prentice-Hall, Engle wood Cliffs, NJ, 1989.
34. Pilling, M.J.; In *Modern Gas Kinetics*, Pilling, M.J.; Smith, I.W.M., eds., Blackwell, Oxford, 1987.
35. Hirst, D.M. In *A Computational Approach to Chemistry*, Blackwell Scientific Publications, Oxford, 1990.
36. Turányi, T. *J. Math. Chem.* **1990**, *5*, 203.
37. Turányi, T.; Bérces, T.; Vajda, S. *Int. J. Chem. Kinet.* **1989**, *21*, 83.
38. Vajda, S.; Valko, P.; Turányi, T. *Int. J. Chem. Kinet.* **1985**, *17*, 55.
39. Gelinas, R.J. Science Applications, Inc., Preprint No AI/PL/C*279*, 1979.
40. Kee, R.J.; Grear, J.F.; Smooke, M.D.; Miller, J.A. Sandia National Labs., SAND 85-8240, 1985.
41. Gardiner, Jr., W.C. *J. Phys. Chem.* **1977**, *81*, 2367.
42. Carter, W.P.L.; Tuazon, E.C.; Ashmann, S.M.; In *Investigation of the Atmospheric Chemistry of Methyl tert-butyl ether (MTBE)*, prepared for the Auto/Oil Air Quality Improvement Research Program, January, 1991.
43. Turányi, T. *Comp. Chem.* **1990**, *14*, 253-254.